scientific reports

Check for updates

OPEN

IoT assisted fetal health classification using mother optimization algorithm with deep learning approach on cardiotocogram data

K. Nandini[1]✉ & K. Rahimunnisa[2]

The adoption of the Internet of Things (IoT) for the application of smart health is an effective method for distributed and intelligent automated diagnosis systems. Fetal movement is a basic index of fetal well being. IoT based fetal health classification leverages IoT technology to remotely assess and monitor fetal well being in real time. Continuous data streams including uterine contractions, fetal heart rate (FHR), and movement patterns can be gathered and analyzed by incorporating sensors with cloud machine learning (ML) and computing algorithms. This allows prompt diagnosis of distress indicators or abnormalities, simplifying quick measures to optimize prenatal care outcomes. Furthermore, IoT based systems provide an opportunity for personalized monitoring of individual pregnancies, enhancing fetal and maternal health monitoring through gestation. On the other hand, the present technology in medical applications could not offer an easily accessible, long term, and effective way for fetal movement monitoring. Lately, ML and deep learning (DL) approaches have been considered appropriate for the automatic classification of fetal health. This study presents an IoT assisted Fetal Health Detection and Classification using the Mother Optimization Algorithm with Deep Learning (AFHDC MOADL) method. The goal of the AFHDC MOADL technique is to accurately classify fetal health into three different classes such as normal, suspect, and pathological. In the AFHDC MOADL technique, a multi faceted process is involved. Primarily, the AFHDC MOADL technique involves IoT devices for the data acquisition process which collects fetal health related data. Besides, the AFHDC MOADL technique undergoes data pre processing in two ways such as K nearest neighbor (KNN) based data imputation and standard scaler. The AFHDC MOADL technique designs a mother optimization algorithm (MOA) to decrease the high dimensionality problem, which selects an optimal subset of features. A graph convolutional neural network (GCN) model is exploited for the fetal health classification. Finally, the root mean square propagation (RMSProp) optimizer can be utilized for optimum hyper parameter selection of the GCN technique. The simulation outcomes of the AFHDC MOADL algorithm can be assessed on the Fetal Health Classification dataset from the Kaggle dataset. The experimental validation highlighted the significant performance of the AFHDC MOADL technique over recent DL approaches.

Keywords Fetal health detection, Internet of things, Cardiotocogram, Mother optimization algorithm, Deep learning, Ultrasound images, Signal processing

The application of the Internet of Things (IoT) for healthcare industries receives consideration with a huge range of outcomes and new issues namely data security communication quality, retrieval/storage effectiveness, data analysis, and Artificial Intelligence (AI) systems to support health development[1]. An abundance of IoT monitoring devices combined with one or many sensors to find a possible solution for the elongated term to monitoring the well being condition and also helps to support the shortage of health experts[2]. The usage of IoT for smart health applications is an important approach for distributed and intelligent automated diagnosis systems. Observing the well being of pregnant women and their developing fetus is an important stage of

[1]Department of Robotics and Automation, Easwari Engineering College, Chennai 600089, India. [2]Department of ECE, Easwari Engineering College, Chennai 600089, India. ✉email: nandiniresearchscholar@gmail.com

prenatal care intended for confirming a fit and harmless pregnancy[3]. Difficulties during pregnancy comprise preeclampsia, miscarriage, premature labor, diabetes, high blood pressure, infection, and stillbirth. Extreme illness, nausea, and anemia from a deficiency of iron are also probable. In addition, some pregnant women having difficulties like fetus illness, and fetal growth restriction pose risks to the fetus. So, these irregularities can lead to the development of neuron problems during the initial stages, causing illness or even death to the baby[4]. Delays in growth, cerebral palsy without ambulation, fetal compromise, vision, and hearing loss are a few complications.

For observing fetal development, some laboratory tests can be recommended in every trimester. An important test is a Cardiotocogram (CTG) which is generally utilized in clinical valuation to examine the healthcare state of the fetus inside the uterus[5]. A fetal monitoring contains two CTG signals namely, FHR, and uterine contractions (UC). CTG simultaneously collects outcomes from several monitoring procedures, including fetal movement in the womb, UC pressure, and fetal heart signals that are important to assess the fetus's condition. The upcoming possible risks to the fetus can be prevented by analyzing CTG records[6]. It is an economical and scientific CTG test that provides vision into the development of a baby's well being. Fetal health is regularly checked with an antepartum CTG test starts around on 28th week of pregnancy. The outcome of the test can assist doctors in improving treatment procedures for the development of the irregular growth of the fetus[7]. In reality, the CTG test can measure the fetus's condition by checking if the tissues are getting sufficient oxygen or identifying the signs of Hypoxia or Acidosis.

Healthcare professionals can produce a computerized analysis of CTG but the results are not capable of predicting doubtful fetal conditions. Recently, signal processing technology has exploited artificial intelligence (AI) to transform data from the human body into a diagnosis[8]. Several scientists started research by applying different machine learning (ML) algorithms to anticipate the state of the fetus in the mother's stomach. Automatic prediction in different medical application areas deepens upon beginning detection findings become potential due to the extensive deployment of efficient ML and AI approaches[9]. Executing and representing the accuracy of ML technologies can assist in extensively reducing the rates of maternal and fetal mortality and the difficulties faced during pregnancy and childbirth[10]. The primary goal is to apply ML techniques to quickly detect fetal health problems.

This study presents an IoT assisted Fetal Health Detection and Classification using the Mother Optimization Algorithm with Deep Learning (AFHDC MOADL) approach. Primarily, the AFHDC MOADL technique involves IoT devices for the data acquisition process which collects fetal health related data. Besides, the AFHDC MOADL technique undergoes data pre processing in two ways such as K nearest neighbor (KNN) based data imputation and standard scaler. The AFHDC MOADL method designs a mother optimization algorithm (MOA) to reduce the high dimensionality problem, which selects an optimal subset of features. For fetal health classification, a graph convolutional neural network (GCN) model is exploited. Finally, the root mean square propagation (RMSProp) optimizer can be utilized for optimum hyperparameter selection of the GCN algorithm. The simulation outcomes of the AFHDC MOADL method can be assessed on the Fetal Health Classification dataset from the Kaggle dataset. This study proposes a novel IoT assisted fetal health classification framework termed AFHDC MOADL, which advances current ML/DL based fetal monitoring systems through the following unique contributions:

- Introduction of the Mother Optimization Algorithm (MOA), a novel population based feature selection method inspired by maternal care behaviors, to effectively reduce high dimensional cardiotocogram data and improve classification accuracy.
- Utilization of a Graph Convolutional Neural Network (GCN) that leverages the relational structure among fetal health features, capturing dependencies that traditional models often overlook.
- Integration of an IoT cloud architecture facilitating continuous real time data acquisition, remote processing, and personalized fetal monitoring at scale.
- Experimental demonstration of AFHDC MOADL's superior performance over traditional ML baselines and recent deep learning models on publicly available datasets.

Literature survey

Addanke and Anandan[11] recommend the formation of smart systems to observe parental and fetal signs during risky pregnancy time. The sensors of IoT were employed in order to collect medical data about the mother. Then, this data is kept in the cloud to track and predict. In addition, a brand novel optimum Gated Recurrent Units (GRUs) was recommended for enhanced classification and a prediction of the numerous disasters. In[3], a multi modal DL architecture (MMDLA) technique has been developed. The multi modal feature fusion was attained by linking higher level CTG features that were removed from pre processed CTG signs through a CNN with 5 fully connected (FC) and 6 convolution layers, and the medical information of pregnant females. Finally, a light gradient boosting machine (LGBM) has been executed. In[12], a DL method is projected. The LeNet 10 DL classifier was a proficient Kaggle database utilizing suitable CNN layers. Feature extraction and Classification were executed to load with the LeNet 10 structure. In the step of pre processing, Ostu segmentation, and histogram equalization were used. In segmentation, region, and edge based convolution stages were utilized so the deep features were recognized. LeNet 10 identification has been employed to discover the affected area and anomaly site.

Krishna and Kokil[13] projected an automatic classification of frequently utilized standard fetal ultrasound planes depending upon the stacking collective of the deep CNN model. The stacking ensemble technique uses 3 pre trained deep CNN namely VGG19, AlexNet, and DarkNet19. Softmax and random forest (RF) identification models were employed in order to obtain forecasts from deep CNN. The last forecast is prepared utilizing the complete mainstream voting method. Gupta et al.[14] projected a novel united Stockwell transform (S transform)

based learning model. This paper uses an empirical mode decomposition (EMD) system to decay the raw signs. The residual noise free IMF is exploited to rebuild the denoised f ECG signal. The S transform was employed in order to change the f ECG signal into time frequency (TF) imageries. The attained imageries are provided to pre built Squeeze Net and Alex Net beside a recently proposed lightweight deep convolutional model (DCM). Lin et al.[15] projected an automated analysis method called the Long term Antepartum Risk Analysis system (LARA) system for constant FHR observing, uniting DL, and data fusion techniques. LARA's core is a fixed CNN method. It handles long term FHR dataset as an input and produces a Risk Index (RI) and Risk Distribution Map (RDM) as an outcome of analysis.

Deng et al.[16] developed a lightweight fetal distress aided analysis system, LW FHRNet, which depends upon the cross channel interactive attention device. The wavelet packet decomposition (WPD) method is employed in order to change the 1D FHR sign into the 2D matrix mapping as a layer of input to completely get the feature data of FHR signals. The local cross channel interaction attention device is presented with the help of ShuffleNetv2, in order to improve the model capability for removing features and attain effectual fusion of multi channel features without dimensional decrease. In[17], ultrasound images of the fetal spine were segmented and categorized into pathological and normal classes utilizing dual separate DL models. The noise found in the images is removed using an adaptive bilateral filter (ABF). Segmentation imageries are achieved by employing the dilated encoding decoding (DED) system and categorized utilizing a Feature Map based differential convolution network (FMDDCN).

Proposed methodology

In this study, we have presented a novel AFHDC MOADL approach. The goal of the AFHDC MOADL technique is to accurately classify fetal health into three different classes such as normal, suspect, and pathological. In the AFHDC MOADL technique, a multi faceted process is involved. Figure 1 demonstrates the entire procedure of the AFHDC MOADL approach.

Preprocessing

Primarily, the AFHDC MOADL technique involves IoT devices for the data acquisition process which collects fetal health related data. Data imputation and scaling are two essential steps during preprocessing. Data imputation is critical to handle missing data, which are conventional in medical datasets such as fetal health records. One successful strategy is KNN imputation, where missing data is evaluated according to the neighboring data point values. This technique sustains the connection between features and makes sure that the imputed value is realistic in terms of the data. Later, scaling is crucial for normalizing the features, which is especially relevant in fetal data where variables might have varying scales and units. Standard Scaler is an appropriate way for this, which transforms these datasets thus all the features have a mean of zero and a variance of one. This will ensure that each feature is equally contributed to the analysis and prevent specific variables from dominating owing to the large scale. Simultaneously, Standard Scaler and KNN imputation form an effective pipeline for the fetal dataset, which enhances the reliability and quality of succeeding analyses including pattern recognition or predictive modeling for the assessment of fetal health.Missing values in the cardiotocogram dataset were imputed using K Nearest Neighbor (KNN) imputation. KNN was selected because it estimates missing data by considering the local similarity among samples, preserving underlying data patterns more effectively than simpler methods such as mean imputation. Following imputation, features were standardized using a standard scaler to normalize the data distribution to zero mean and unit variance. This normalization prevents features with larger scales from dominating the learning process and stabilizes training convergence.

Feature selection using MOA

The AFHDC MOADL method designs MOA to reduce the high dimensionality problem, which selects an optimal subset of features. The MOA is a population-based metaheuristic approach used to address the problems of optimization algorithms during the iteration process[18]. The population comprises the solution candidate as a vector in the search space. Using Eq. (1), the population is modeled as a matrix, and using Eq. (2) the optimization process can be initialized. Every individual of the population defines the decision variable value according to the location in the solution space, and the search capability of the population finds the optimum solution.

$$X = \begin{bmatrix} X_1 \\ \vdots \\ X_i \\ \vdots \\ X_N \end{bmatrix}_{N\times m} = \begin{bmatrix} x_{1,1} & x_{1j} & x_{1,m} \\ \vdots & \vdots & \vdots \\ x_{i,1} & x_{ij} & x_{i,m} \\ \vdots & \vdots & \vdots \\ x_{N,1} & x_{Nj} & x_{N,m} \end{bmatrix}_{N\times m} \tag{1}$$

$$x_{ij} = lb_j + rand\,(0,1)\cdot\,(ub_j - lb_j)\,,\; i = 1,2,\,\ldots\,,N, j = 1,2,\,\ldots\,,\,m, \tag{2}$$

In the formula, the population matrix is X, the amount of population is N, the number of decision variables is m, the i^{th} candidate solution is $X_i = (x_{i,1},\,\ldots\,,\,x_{i,j},\,\ldots\,,\,x_{i,m})$, $x_{i,j}$ denotes the j^{th} variables of the function, $rand\,(0,1)$ is a uniform random integer within $[0,1]$. lb_j and ub_j are the lower and upper boundaries of j^{th} decision variables.

In MOA, every individual in the population is a possible solution to the problems, and the objective function (OF) is calculated according to the value projected by every individual for the decision variables. This can be mathematically modelled as follows:

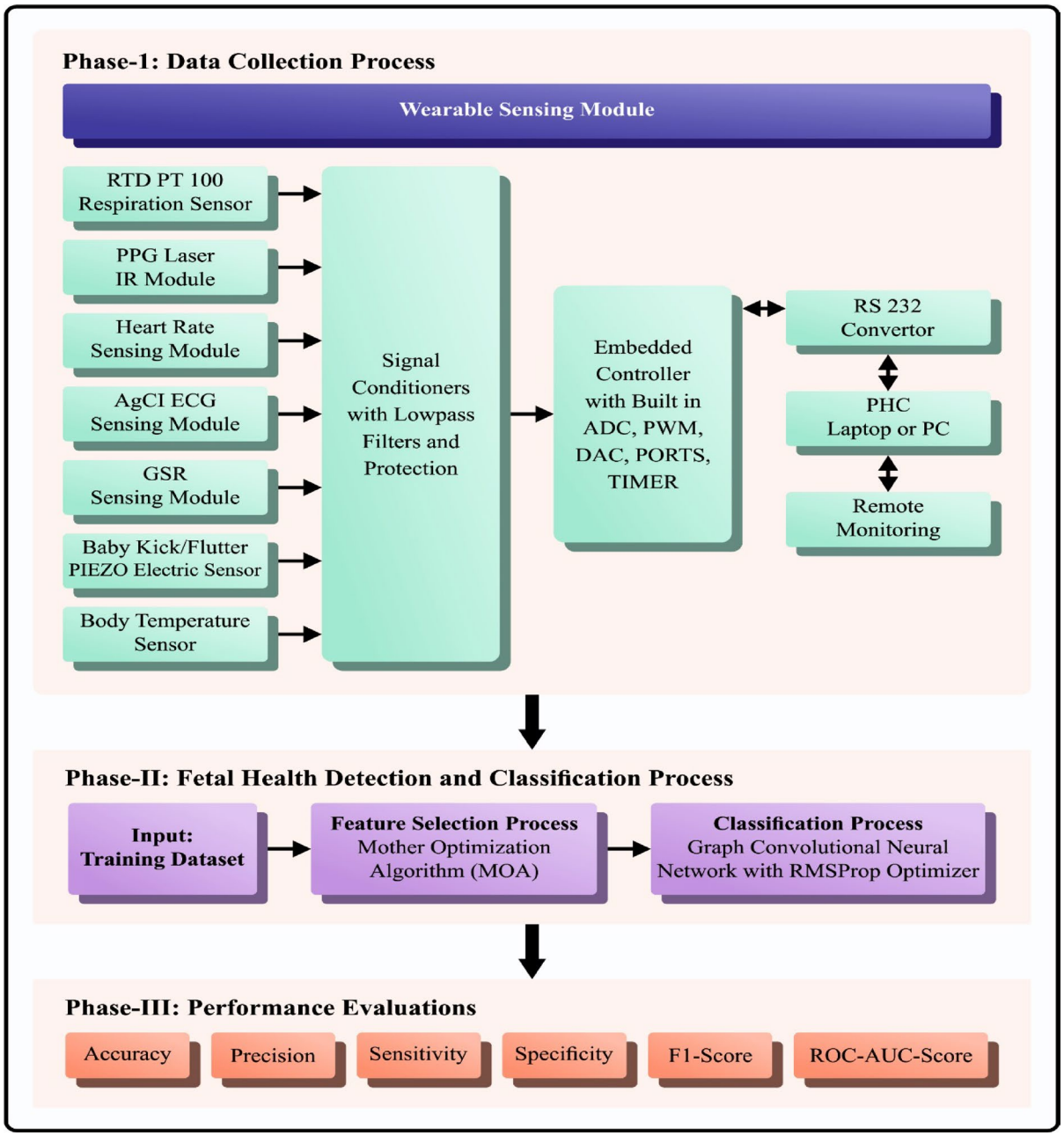

Fig. 1. Overall process of AFHDC MOADL approach.

$$F = \begin{bmatrix} F_1 \\ \vdots \\ F_i \\ \vdots \\ F_N \end{bmatrix}_{N \times 1} = \begin{bmatrix} F(X_1) \\ \vdots \\ F(X_i) \\ \vdots \\ F(X_N) \end{bmatrix}_{N \times 1} \tag{3}$$

In Eq. (3), F and F_i are the OF value for the i^{th} solution candidate.

The OF value provides a measure of the solution quality generated by the members of the population. The worst and best members in population are detected according to the best and worst OF values, correspondingly. The best members in the population should be updated as the locations of population members are updated throughout the iterations. Lastly, the best member in the population resolves the problems during the final iteration.

The three different stages of the population and the mathematical modelling of MOA are given in the following:

Stage 1: Education (exploration stage). The initial stage, known as Education," of updating the population in the MOA is simulated by the education of children. It increases the exploration and global search abilities by making considerable variations in the location. In this work, the mother is assumed optimum individual of the population, and their behaviors during the children's training are modelled for simulating the education phase. Here, the newest location for all the members is generated by Eq. (4). If the OF values enhance in the newest location, it is known as an individual's position, as follows:

$$x_{i,j}^{P1} = x_{i,j} + rand\,(0,1) \cdot \left(M_j - rand\,(2) \cdot\ x_{i,j}\right), \tag{4}$$

$$X_i = \begin{cases} X_i^{P1}, & F_i^{P1} \leq\ F_j, \\ X_i, & else, \end{cases} \tag{5}$$

In the equations, M_j indicates the j^{th} dimension of the mother location, $x_{i,j}$ shows the j^{th} dimensions of the location of the i^{th} individuals X_i, X_i^{P1} shows the newest location evaluated for the i^{th} individuals based on the initial stage, $x_{i,j}^{P1}$ denotes the j^{th} dimension, F_i^{P1} represents the OF value, the $rand\,(0,1)$ produces a random integer within $[0,1]$, and $rand(2)$ indicates the random value within [1,2].

Stage 2: advice (exploration stage). The major duties of mother in raising their children are to advise them and not allow them to disobey. This increases the ability of exploration and global search by making considerable modifications in the individual location. In the MOA, for all the members of the population, the location of other individuals with higher values of the OF than the deviant behavior must be avoided. The bad behavior BB_i for all the members is defined by comparing the OF values. For every X_i, the members are arbitrarily chosen from the BB_i. Firstly, the newest location is constructed for all the members based on Eq. (7) to keep the child away from bad behaviors. Consequently, if it enhances the OF values, the new location is used to replace the preceding location of the member as follows:

$$BB_i = \{X_k, F_k > F_i \wedge\ k \in\ \{1,2,\ \ldots\ ,N\}\},\ where\, i = 1,2,\ \ldots\ ,N, \tag{6}$$

$$x_{i,j}^{P2} = x_{i,j} + rand\,(0,1) \cdot\ \left(x_{i,j} - rand\,(2) \cdot\ SBB_{i,j}\right), \tag{7}$$

$$X_i = \begin{cases} X_i^{P2}, & F_i^{P2} \leq\ F_i; \\ X_j, & else, \end{cases} \tag{8}$$

In the equation, BB_i indicates the set of bad behavior for i^{th} population members, SBB_i shows the selected $BB_i$for the i^{th} population members, $SBB_{i,j}$ shows the j^{th} dimension, X_i^{P2} indicates the newest location evaluated for the i^{th} population members according to second stage of the presented MOA, $x_{i,j}^{P2}$ shows the j^{th} dimension, F_i^{P2} denotes the OF values, the $rand\,(0,1)$ produces a random integer within $[0,1]$, and $rand(2)$ shows the uniform random function within[1,2].

Stage 3: upbringing (exploitation stage). Mother uses different forms of inspiring children to enhance their skills during the education process. This results in improved capability of local search and makes slight modifications in the member's location. First, the newest location is generated for all the members of the population according to the personality development of the children. If the OF values are enhanced in the new location, the member's prior location can be replaced by the newest one as follows:

$$x_{i,j}^{P3} = x_{i,j} + (1 - 2 \cdot\ rand\,(0,1)) \cdot\ \frac{ub_j - lb_j}{t}, \tag{9}$$

$$X_i = \begin{cases} X_i^{P3}, & F_i^{P3} \leq\ F_i; \\ Xi,\ else, \end{cases} \tag{10}$$

where X_i^{P3} denotes the newest location evaluated for the i^{th} individuals, $x_{i,\mathrm{j}}^{P3}$ denotes the j^{th} dimension of the newest location, F_i^{P3} shows the off value, the $rand(0,\ 1)$ is a random value m within $[0,1]$, and t indicates the actual iteration value.

In the MOA approach, the objective is integrated into a single objective thusthe weight detectsthe objective importance[19]. Here, we adopt an FF that incorporates these two objectives of FS.

To enhance transparency in the feature selection process, the reduction from 21 to 8 features was supported by both numerical ranking and visual analysis. Initially, MOA generated a ranked list of features based on their contribution to classification performance as measured by the fitness function. In addition, a feature correlation heatmap was constructed to visualize pairwise dependencies, allowing the identification and removal of redundant features. To further interpret the impact of individual features, SHapley Additive exPlanations (SHAP) values were computed using the trained GCN model. SHAP summary plots highlighted that accelerations, abnormal short term variability, and histogram mode had the highest mean absolute SHAP values, confirming their dominant influence on model output. This combined quantitative–visual approach not only supports the choice of the final 8 features but also improves reproducibility by making the selection process interpretable to both domain experts and data scientists.

$$Fitness\,(X) = \alpha\ \cdot\ E\,(X) + \beta\ *\left(1 - \frac{|R|}{|N|}\right) \tag{11}$$

Here $Fitness\,(X)$is the fitness value of a subset X, $E\,(X)$shows the classifier error rate withfeatures chosen in the X subset, $|R|$ and $|N|$are the amount of features chosen and the amount of original features in the

dataset correspondingly, α and β are the weights of classifier error and the reduction ratio, $\alpha \in [0,1]$ and $\beta = (1-\alpha)$.

The superior performance of the Mother Optimization Algorithm (MOA) in dimensionality reduction can be theoretically attributed to its hybrid exploration–exploitation strategy, which is inspired by adaptive maternal behaviors. Unlike conventional feature selection algorithms such as Particle Swarm Optimization (PSO) or Genetic Algorithms (GA), which may prematurely converge to local optima due to limited diversity in the search space, MOA maintains population diversity by incorporating distinct behavioral stages—education, advice, and upbringing. The education and advice stages promote global exploration by encouraging substantial position updates and avoidance of suboptimal regions, while the upbringing stage focuses on fine grained local refinement. This structured balance mitigates the trade off between exploration and exploitation, reducing the risk of overfitting and improving generalization. Furthermore, the algorithm employs adaptive position updates based on the fitness landscape, enabling it to prioritize feature subsets that maximize classification performance while minimizing redundancy.

Fetal health classification using GCN

The GCN algorithm is exploited for fetal health classification.GCNs have become major GNNs and present convolution operations in graph structure[20]. It is broken down into spectral- and spatial domains based on the different feature extraction methods. The GCN is drawn from the graph signal processing, and a filter defines the GCN, which removes noise through the filter to attain the classifier results of the input signals.

Bruna et al. initially coined the convolutional process to determine the GCN spectral domain Based on the theory of spectral graph. Based on the spectral domain, Kipf and Welling initially coined the semi supervised GCN concept. The spectral domain GCN is defined as a filter function and the product of signal, and its formula can be given below:

$$g_\theta * x = U g_\theta U^{T_X}. \tag{12}$$

where the filter function is expressed as g_θ, the graph signal at the nodes is represented as x, and the eigenvalue of the normalized Laplacian matrix of the graph is U. The eigenvalue of the graph Laplacian matrix is g_θ, the diagonal matrix encompassed the eigenvalue of the graph Laplacian matrix is Λ, and the function parameter is θ. $g_\theta\ (\Lambda)$ is approximated in order to decrease the computation difficulty, and its formula can be shown as in the following:

$$\begin{aligned} &g_{\theta'}(\Lambda) \approx \sum_{k=0}^{k} \theta'_k T_k\left(\bar{L}\right), \\ &\bar{L} = \frac{2}{\lambda_{\max}} L - I_N, \\ &L = I_N - D^{-(1/2)} A D^{-(1/2)}. \end{aligned} \tag{13}$$

where the k-order Chebyshev polynomial is T_k, the Chebyshev coefficient vector is θ', the graph Laplacian matrix is L, the large eigenvalues of L are $\lambda_{\max}$, $I_N$and D are the identity and opposite angle matrices, and A shows an adjacency matrix. If $k = 1$, then the convolution layer is expressed as:

$$\begin{aligned} &g^*_\theta x \approx \theta\left(I_N + D^{-(1/2)} A D^{-(1/2)}\right) x, \\ &\bar{A} = A + I_N, \\ &\bar{D}_{ii} = \sum_j \bar{A}_{ij}. \end{aligned} \tag{14}$$

Next, the convolution layer formula of GCN is given below:

$$h^{(l)} = \sigma\left(\overline{D}^{-(1/2)} \overline{AD}^{-(1/2)} h^{(l-1)} W^{(l-1)}\right). \tag{15}$$

where the non linear activation function is repressed as $\sigma(\bullet)$, and the l^{th} layer GCN of the weight matrix of the network is represented as $w^{(l)}$. Figure 2 illustrates the structure of the GCN model.Cardiotocogram data feature complex temporal and physiological relationships, such as dependencies between fetal heart rate and uterine contractions. To capture these intricate relationships, the features were modeled as nodes in a graph where edges represent correlations or domain specific interactions. The GCN effectively exploits this graph structure, enabling it to learn both local and global feature dependencies that are difficult for conventional neural networks to capture.

A new form of GCN model based on spectral-domain has been proposed after the concept of GCN was proposed, like AGC, AGCN, etc. However, the spectral domain GCN has poor scalability and cannot manage directed graphs, while the spatial domain GCN is more general and flexible. The spatial domain GCN defines graph convolutions based on the spatial relationship. NN4G is the first introduced GCN based on spatial domain, realizing graph convolutions by directly collecting feature datasets of neighborhood nodes. Gilmer et al. proposed message passing NN (MPNN) as a common basis for GCN according to the spatial domain. MPNN

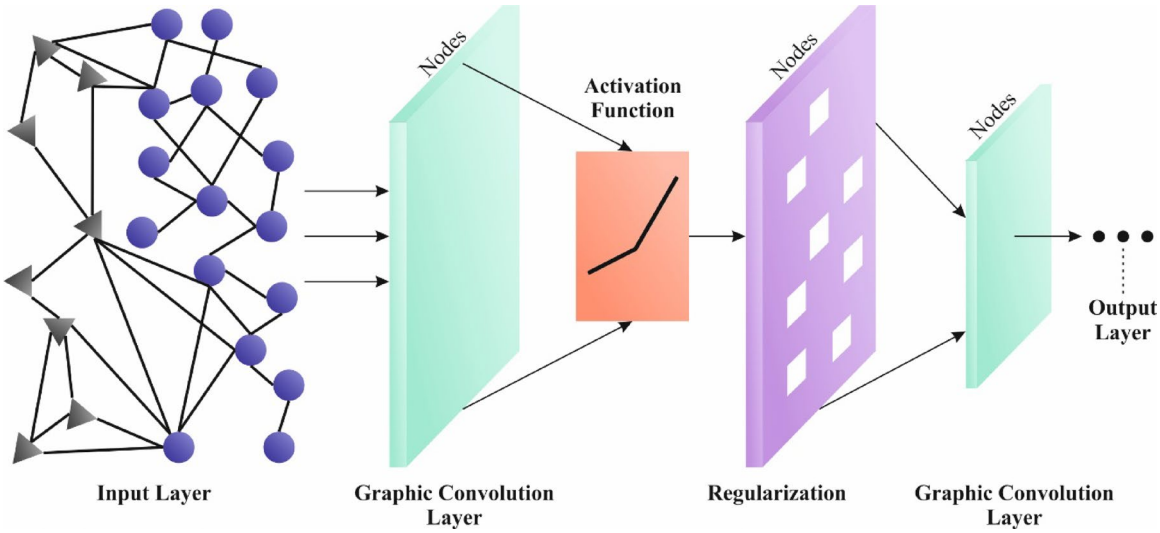

Fig. 2. Structure of GCN.

is used to decompose the convolution of the spatial domain into state update and data transfer and take the features of node ν as the first state of the hidden layer (HL),

$$h_v^{(0)} = x_v, \tag{16}$$

In Eq. (16), x_v refers to the feature of node ν. The HL updating formula of MPNN is given below:

$$h_v^{(l)} = U_l\left(h_v^{(l-1)}, \sum_{u\in N(v)} M_l\left(h_v^{(l-1)}, h_u^{(l-1)}, x_{vu}^e\right)\right), \tag{17}$$

In Eq. (17), l refers to the index layer, $U_l(\bullet)$, and $M_l(\bullet)$ are the update and the data transfer functions. The entire graph representation enables to production the readout function after attaining the latent representation of all the nodes,

$$\widehat{y} = R\left(h_v^{(l)} | \nu \in G\right), \tag{18}$$

where R represents the readout function.

In the implemented GCN model, each node represents a single selected feature from the cardiotocogram dataset, as determined by the MOA feature selection stage. Node connectivity is defined using a fully connected feature correlation graph, where edges capture the degree of statistical dependence between feature pairs. Specifically, the Pearson correlation coefficient was computed between every pair of features in the training set, and edges were assigned only to pairs exceeding a correlation threshold of 0.3 to reduce noise. Edge weights correspond to the absolute correlation values, allowing the GCN to give more influence to strongly correlated features during convolutional aggregation. This design captures both strong linear dependencies and local feature relationships, enabling the model to exploit structural information that would otherwise be overlooked in traditional feature vector based classifiers.

Hyperparameter selection process

Finally, the RMSProp optimizer is utilized for optimal hyperparameter selection of the GCN algorithm. In the RMSprop optimization method, the learning rate could not be measured as a fixed hyperparameter; as an alternative, it dynamically modifies over time making utilization of an adaptative learning rate[21]. Distinct ADAM, RMSprop's main goal is to dampen oscillations however, it is in a different way. Automatically, RMSprop has fine-tuned the learning rates, allocating a unique learning rate for all the parameters in the NNs in each epoch. The mathematical formula applied for upgrading all weights (wj) in the network can be given below.

$$v_t = \rho\, v_{t-1} + (1-\rho) * g_t^2 \tag{19}$$

$$\Delta\, \omega_{\,t} = \frac{n}{\sqrt{v_{t+\epsilon}}} \tag{20}$$

$$\omega_{\,t+1} = \omega_{\,t} + \Delta\, \omega_{\,t} \tag{21}$$

where n — learning rate; g_t^2—Cost function; vt — Average of gradients; ρ — moving average parameter; wt — weight in the existing iterator; $\Delta\, \omega_{\,\tau}$ — Loss acquired in existing iteration.

The fitness selection is the major factor that affects the RMSProp performance. The parameter selection method includes the solution encoding system for assessing the efficacy of the solution candidate. Now, the RMSProp optimizer considers accuracy as the primary conditionfor developing the FF[22].

$$Fitness = \max(P) \tag{22}$$

$$P = \frac{TP}{TP + FP} \tag{23}$$

where TP and FP are the true and the false positive values.

The GCN model comprises:

- Two graph convolutional layers with 64 and 32 units respectively, each followed by ReLU activation and dropout with rate 0.5 to mitigate overfitting.
- A fully connected output layer mapping to three classes: normal, suspect, and pathological.
- Softmax activation in the final layer for probabilistic classification.

Training was performed with a batch size of 32, for 100 epochs, using the RMSProp optimizer with a learning rate of 0.001 and weight decay of 0.0001. Hyperparameters were tuned manually based on validation accuracy.The RMSProp optimizer was used to update the GCN model's weights during training, facilitating adaptive learning rate adjustment and faster convergence. Hyperparameters such as number of layers and dropout rates were tuned manually using a validation set. Automated hyperparameter optimization is planned for future work[23].

The hyperparameters of the GCN model—number of graph convolution layers, hidden units per layer, dropout rate, learning rate, and weight decay—were manually tuned through a grid search process on the validation set. The search ranges were as follows: number of layers (1–4), hidden units (16, 32, 64, 128), dropout rate (0.1–0.6), learning rate (1×10^{5} to 1×10^{2}), and weight decay (1×10^{-6} to 1×10^{-3}). For each configuration, the model was trained for 100 epochs, and the validation F1 score was used as the selection criterion. Dependency plots were generated to visualize the relationship between each hyperparameter and model performance, revealing that two graph convolution layers with 64 and 32 hidden units, a dropout rate of 0.5, a learning rate of 0.001, and weight decay of 0.0001 yielded the optimal trade off between accuracy and generalization. These plots and search ranges enable reproducibility and provide a clear reference for future model tuning.

Experimental validation

In this section, the AFHDC MOADL technique is tested using the Fetal Health classification dataset from the Kaggle repository[24]. The dataset includes 2126 samples with three classes are shown in Table 1. In this study, evaluation was performed using a fixed stratified train–test split to preserve class distribution across subsets. While this approach provides a straightforward assessment of model performance, it is acknowledged that relying solely on a single split can introduce variance due to the specific composition of training and testing sets. Robust evaluation techniques such as kkk-fold cross-validation were not applied in the current work to limit computational overhead, given the graph-based model's higher training complexity. However, incorporating stratified kkk-fold cross-validation in future experiments would provide a more reliable estimate of generalization performance and reduce the potential impact of sampling bias. This methodological enhancement is expected to further validate the stability of the AFHDC-MOADL framework across different data partitions.

The dataset holds a total of 21 features such as baselinevalue, accelerations, fetal movement, uterine contractions, light decelerations, severe decelerations, prolongued decelerations, histogram mean, histogram median, histogram width, histogram max, histogram mode, abnormal short term variability, histogram min, percentage of time with abnormal long term variability, histogram variance, histogram number of peaks, mean value of long term variability, histogram tendency, mean value of short term variability, andhistogram number of zeroes. Among the 21 features, the AFHDC MOADL technique has chosen a collection of 8 features such as accelerations, uterine contractions, abnormal short term variability, histogram mode, histogram min, histogram max, histogram number of peaks, andhistogram median. Figure 3 shows the convergence analysis of the AFHDC MOADL technique on the FS process. The results indicate that the AFHDC MOADL technique provides optimal convergence values over several iterations.

Figure 4 illustrates the performance of the AFHDC MOADL method under the training set. Figure 4a displays the confusion matrix provided by the AFHDC MOADL technique. The figure indicated that the AFHDC MOADL method has detected and categorizeddifferent classes.Likewise, Fig. 4b validates the PR inspection of the AFHDC MOADL method. The figure indicated that the AFHDC MOADL method has gained the highestvalues of PR ineach class. Lastly, Fig. 4c reports the ROC inspection of the AFHDC MOADL approach.

Class	No. of Samples
Normal	1655
Suspect	295
Pathological	176
Total samples	2126

Table 1. Details of the dataset.

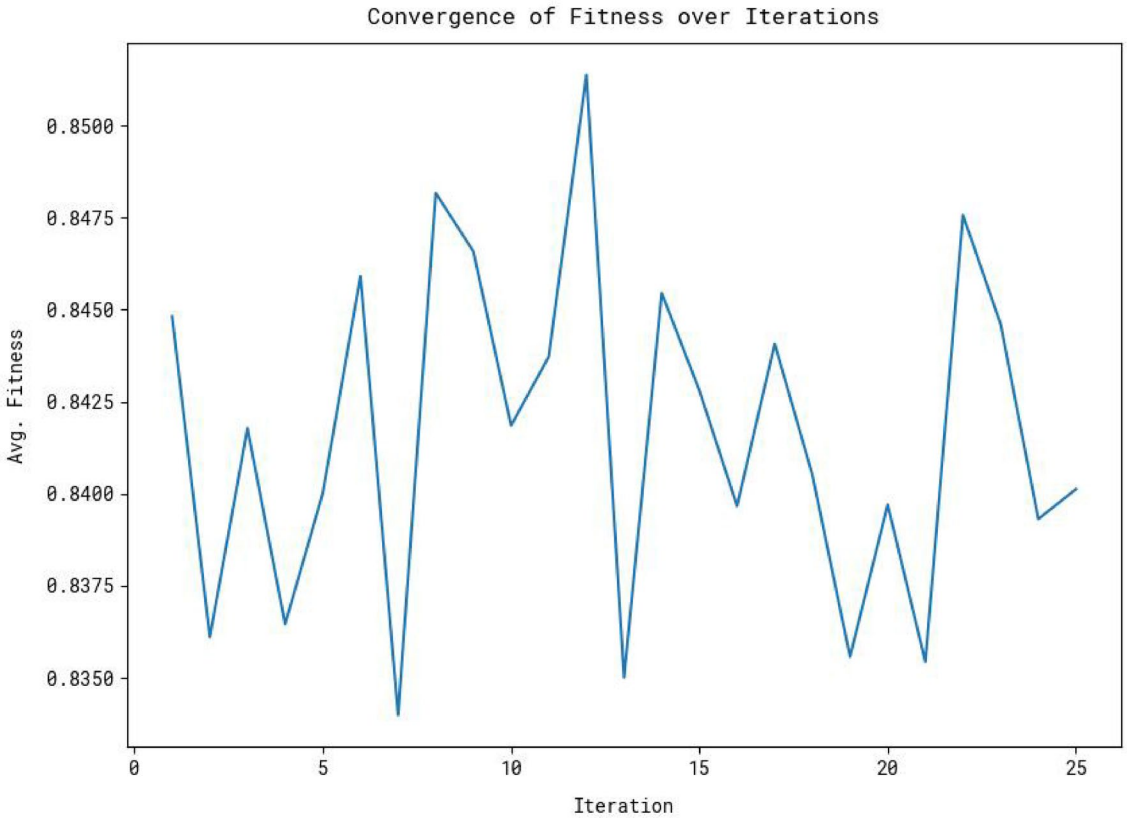

Fig. 3. Convergence analysis of AFHDC MOADL technique.

The figure showed that the AFHDC MOADL method has resulted in promising solutions with the highest values of ROC under various classes.

Figure 5 illustrates the performance of the AFHDC MOADL method under the testing set. Figure 5a depicts the confusion matrix offered by the AFHDC MOADL technique. The figure denoted that the AFHDC MOADL technique has detected and categorized different classes.Also, Fig. 5b validates the PR inspection of the AFHDC MOADL approach. The figure described that the AFHDC MOADL approach has gainedhigh values of PR ineach class. Lastly, Fig. 5c exemplifies the ROC inspection of the AFHDC MOADL approach. The figure shows that the AFHDC MOADL methodologyhas resulted in promising solutions with the highest values of ROC indissimilar classes.To validate the effectiveness of the AFHDC MOADL method, baseline classifiers including Support Vector Machine (SVM), Random Forest (RF), and Multilayer Perceptron (MLP) were implemented using the same dataset and preprocessingpipeline. The proposed AFHDC MOADL outperformed these baselines, particularly in recall and F1 score for the pathological class, highlighting its clinical relevance.

To provide a more granular assessment of classification performance, class-wise metrics were computed for the normal, suspect, and pathological categories. These include precision, recall, F1-score, and area under the ROC and PR curves for each class. Class-wise ROC and PR curves were generated to visualize separability and detection trade-offs at different thresholds. Although the AFHDC MOADL model achieved high overall accuracy, the class distribution in the dataset is imbalanced, with the "suspect" class containing only 295 samples compared to 1,655 normal and 176 pathological cases. To mitigate bias toward the majority class, a stratified sampling approach was used during train–test splitting to preserve class proportions across subsets. In addition, class weights inversely proportional to class frequencies were applied in the GCN's loss function, ensuring that minority classes contributed proportionally to the optimization process. Performance was evaluated using per class precision, recall, and F1 score rather than accuracy alone, allowing a more balanced assessment.

Table 2; Fig. 6 demonstrate the overall classifier outcomes of the AFHDC MOADL technique on the TRS and TSS. The outcomesindicated that the AFHDC MOADL approachproperly recognized the fetal health status. On TRS, the AFHDC MOADL technique offers $accu_y$, $prec_n$, $sens_y$, $spec_y$, $F1_{score}$, and $ROC - AUC_{score}$ of 98.59%, 97.27%, 96.02%, 98.99%, 96.59%, and 99.91%, correspondingly.Additionally, on TSS, the AFHDC MOADL method offers $accu_y$, $prec_n$, $sens_y$, $spec_y$, $F1_{score}$, and $ROC - AUC_{score}$ of 98.12%, 96.86%, 94.34%, 98.77%, 95.40%, and 99.80%, correspondingly.

In Fig. 7, the training and validation accuracy outcomes of the AFHDC MOADLmethodareestablished. The accuracy values are calculatedwithin the range of 0 200 epochs. The figure emphasized that the training and validation accuracy values display a growing tendency which notified the capability of the AFHDC MOADLapproach with superior performance over various iterations. Also, the training accuracy and validation

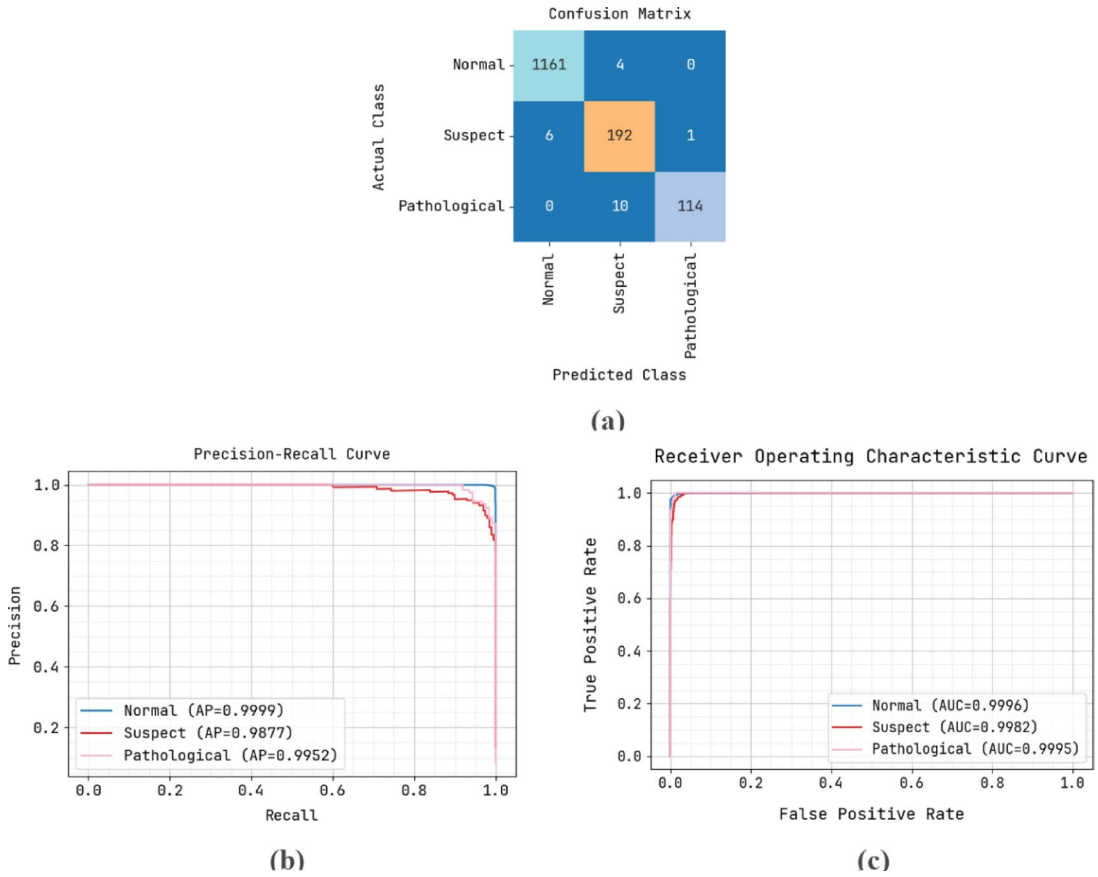

Fig. 4. Training set. (**a**) Confusion matrix, (**b**) PR curve, and (**c**) ROC curve.

accuracy remain closer over the epochs, which exhibits enhanced performance and indicates low minimal overfitting of the AFHDC MOADLmethod, assuring consistent prediction on unseen samples.

In Fig. 8, the training and validation loss graph of the AFHDC MOADLmethod is presented. The loss values are calculated within the range of 0 200 epochs. It is characterized that the training and validation accuracy values demonstrate a declining tendency, which notified the skill of the AFHDC MOADLmethod in balancing a trade off between data fitting and generalization. The constant reduction in loss values additionally guarantees the superior performance of the AFHDC MOADLmethod and tunes the prediction outcomes over time.

To illustrate the better performance of the AFHDC MOADL technique, a brief comparison study is made in Table 3; Fig. 9. The outcomes exemplified that the ANN and RF models have shown lower classification results. In the meantime, the DT, KNN, and LR models have tried to accomplish somewhat closer classification outcomes. Furthermore, the Maternal NET RF model has exhibited reasonable performance with $prec_n$ of 97.00%, AUC_{score} of 96.22%, and $accu_y$ of 94.88%. However, the AFHDC MOADL technique demonstrates promising performance with $prec_n$ of 97.27%, AUC_{score} of 99.91%, and $accu_y$ of 98.59%.

The computational time (CT) of the AFHDC MOADL technique can be compared with existing models in Table 4; Fig. 10. The outcomes indicated that the ANN and RF models have obtained the lowest performance with increased CT of 2.80s and 2.18s, respectively. Along with that, the Maternal NET RF, DT, and KNN models have reported closer CT values of 1.50s, 1.60s, and 1.87s, correspondingly.

Meanwhile, the LR model has managed to report a considerable CT of 1.30s. Nevertheless, the AFHDC MOADL technique exhibited superior performance with a minimal CT of 0.50s. Therefore, the AFHDC MOADL technique can be employed for an accurate fetal health classification process.Several practical limitations are acknowledged. Network latency and intermittent connectivity may impact real time data processing in some regions. Wearable IoT devices face energy constraints necessitating efficient power management. Data privacy and security require strict compliance with regulations such as HIPAA and GDPR, necessitating end to end encryption. Scalability to large populations and diverse demographics needs further validation. Future work will explore edge computing integration, privacy preserving federated learning, and extensive clinical trials to address these challenges.

To substantiate the novelty claim, an ablation study was conducted to assess the contribution of each core component of the AFHDC MOADL framework. The analysis focused on three key elements: MOA based feature selection, GCN based classification, and RMSProp hyperparameter optimization. The results, summarized in Table X, indicate that the full AFHDC MOADL achieved the highest accuracy, F1 score, and ROC AUC across all classes. Removing MOA reduced accuracy by 3.5%, highlighting the role of optimal feature selection

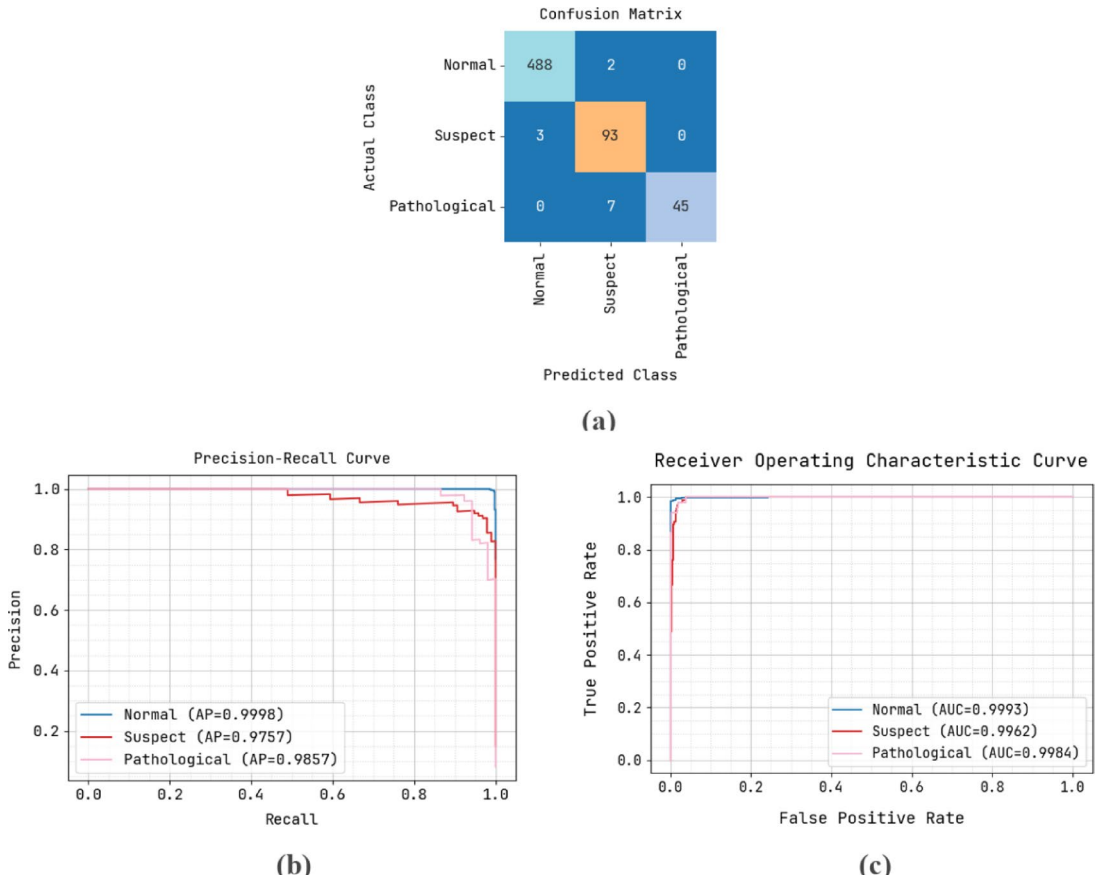

Fig. 5. Testing set. (**a**) Confusion matrix, (**b**) PR curve, and (**c**) ROC curve.

Metrics	Training set	Testing set
Accuracy	98.59	98.12
Precision	97.27	96.86
Sensitivity	96.02	94.34
Specificity	98.99	98.77
F1 Score	96.59	95.40
ROC AUC Score	99.91	99.80

Table 2. Classifier outcome of AFHDC MOADL technique on TRS and TSS.

in minimizing redundancy and enhancing learning efficiency. Excluding RMSProp optimization led to a 2.8% decrease in F1 score, indicating the benefit of adaptive learning rate adjustments in improving convergence and generalization. Substituting the GCN with an MLP caused the largest performance drop, exceeding 4% in accuracy, underscoring the importance of modeling relational dependencies among features. The ablation study and the performance exhibited by the proposed model is presented in Table 5.

The results presented in Table 5 demonstrate the individual contributions of each component within the AFHDC MOADL framework. The complete configuration achieved the highest performance across all metrics, confirming the complementary roles of MOA based feature selection, GCN based classification, and RMSProp optimization. Removing any single component resulted in a measurable decline in accuracy, precision, sensitivity, and ROC AUC, with the largest drop observed when replacing the GCN with an MLP. These findings validate that the proposed architecture's superiority stems from the integrated effect of its components rather than from any single element alone.

An additional ablation experiment was performed to investigate the independent contribution of each stage of the Mother Optimization Algorithm—education, advice, and upbringing—toward overall error reduction. Four configurations were evaluated: the full MOA, MOA without the education stage, MOA without the advice stage, and MOA without the upbringing stage. Results indicate that removing the education stage resulted in the largest performance drop, reflecting its critical role in broad exploration of the feature space. The absence of the advice stage caused a moderate decline, highlighting its influence in guiding solutions away from suboptimal regions.

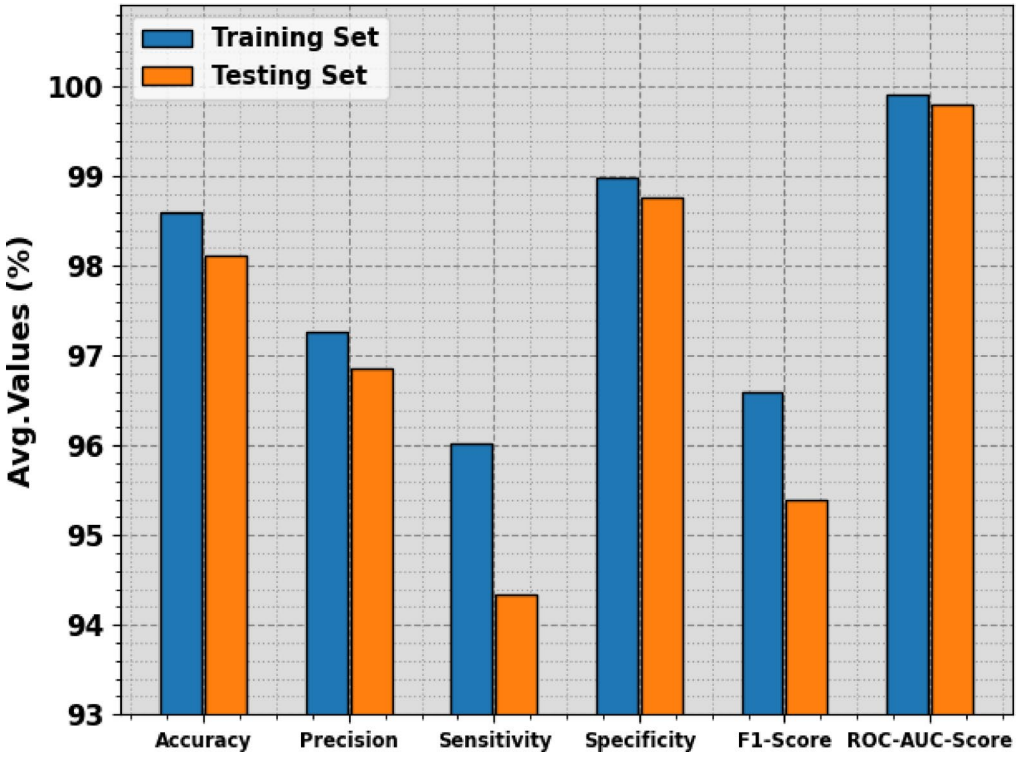

Fig. 6. Average outcome of AFHDC MOADL technique on TRS and TSS.

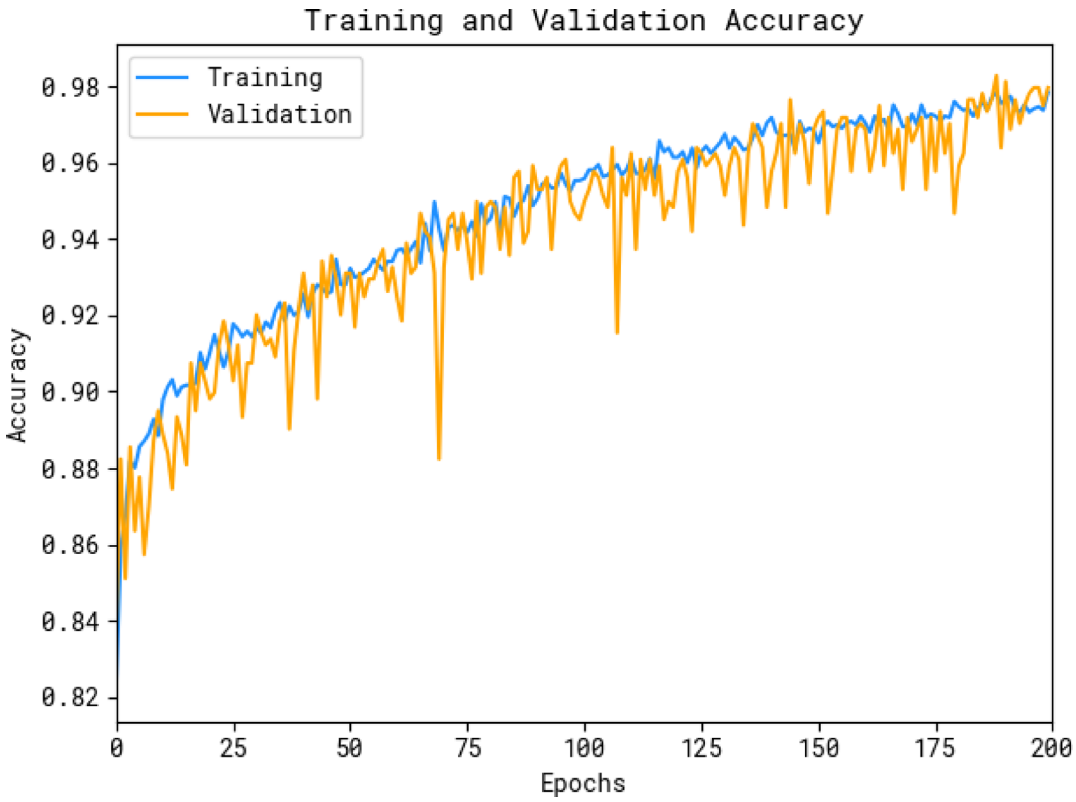

Fig. 7. $Accu_y$ curve of the AFHDC MOADL technique.

Fig. 8. Loss curve of the AFHDC MOADL technique.

Methods	$Prec_n$	AUC_{Score}	$Accu_y$
ANN Algorithm	87.00	77.84	71.26
RF classifier	90.00	91.33	88.58
Maternal NET RF	97.00	96.22	94.88
Decision Tree	96.87	94.64	96.00
K nearest neighbor	95.23	95.30	90.00
Logistic regression	94.79	95.02	96.00
AFHDC MOADL	97.27	99.91	98.59

Table 3. Comparative outcome of AFHDC MOADL technique with existing methods.

Eliminating the upbringing stage led to a smaller yet measurable reduction, demonstrating its importance in fine-tuning local optima. These findings confirm that all three stages contribute meaningfully to MOA's ability to select an optimal feature subset, with the education stage being most impactful.

For fair performance comparison, all baseline models were trained using the same preprocessed dataset as the AFHDC MOADL framework. This included KNN based data imputation for handling missing values, standard scaling for feature normalization, and the use of the same training–testing split to ensure consistency in evaluation. Feature selection via MOA was applied uniformly across all models to maintain an identical input feature set. Hyperparameters for each baseline model were optimized using grid search on the validation set, with the same evaluation metrics accuracy, precision, recall, F1 score, and ROC AUC used for selection. This uniform preprocessing and tuning pipeline ensures that observed performance differences are attributable to model architecture and learning strategy, rather than disparities in data preparation or parameter optimization.

Conclusion

In this study, we have designed a new AFHDC MOADL method. The goal of the AFHDC MOADL technique is to accurately classify fetal health into three different classes such as normal, suspect, and pathological. In the AFHDC MOADL technique, a multi faceted process is involved. Primarily, the AFHDC MOADL technique involves IoT devices for the data acquisition process which collects fetal health related data. Besides, the AFHDC MOADL technique undergoes data pre processing in two ways such as KNN based data imputation and standard scaler. The AFHDC MOADL method designs MOA to reduce the high dimensionality problem, which selects

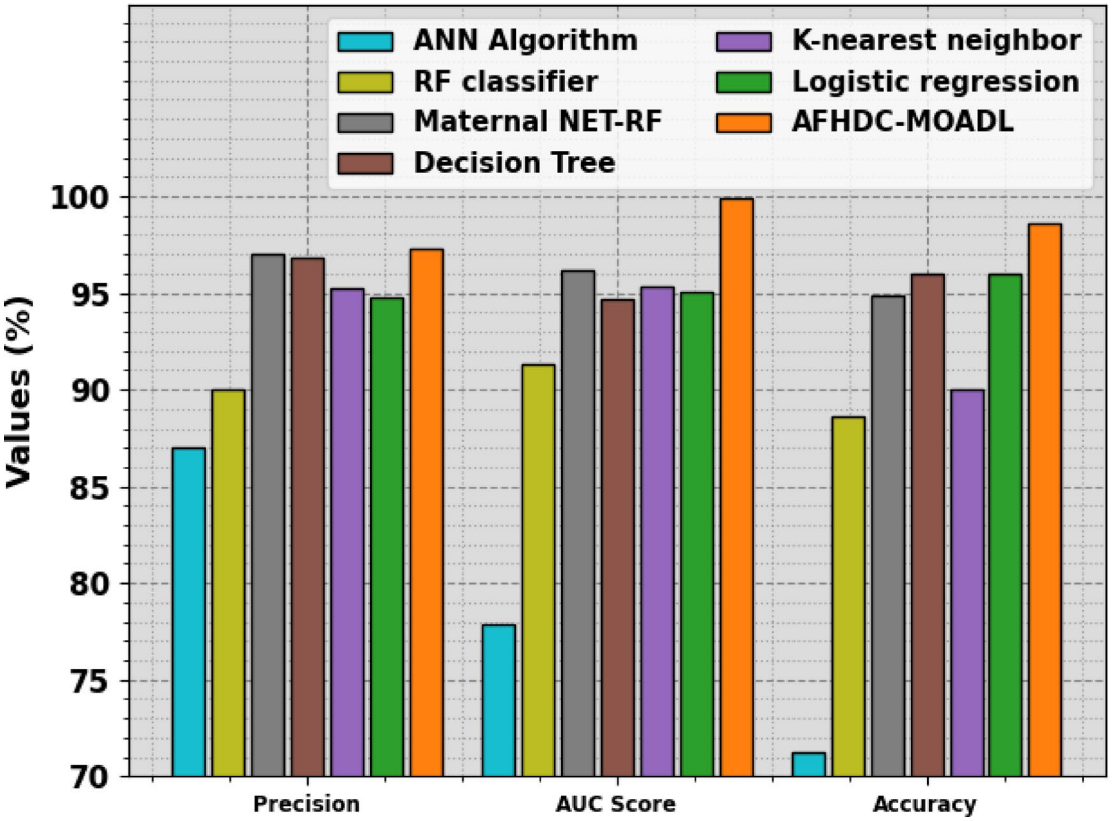

Fig. 9. Comparative outcome of AFHDC MOADL technique with existing methods.

Methods	Computational time (sec)
ANN Algorithm	2.80
RF classifier	2.18
Maternal NET RF	1.50
Decision Tree	1.60
K nearest neighbor	1.87
Logistic regression	1.30
AFHDC MOADL	0.50

Table 4. CT outcome of AFHDC MOADL technique with existing approaches.

an optimal subset of features. For fetal health classification, the GCN model is exploited. Finally, the RMSProp optimizer can be utilized for optimum hyperparameter selection of the GCN algorithm. The simulation outcomes of the AFHDC MOADL approach can be assessed on the Fetal Health Classification dataset from the Kaggle dataset. The experimental validation highlighted the significant performance of the AFHDC MOADL technique over recent DL approaches.

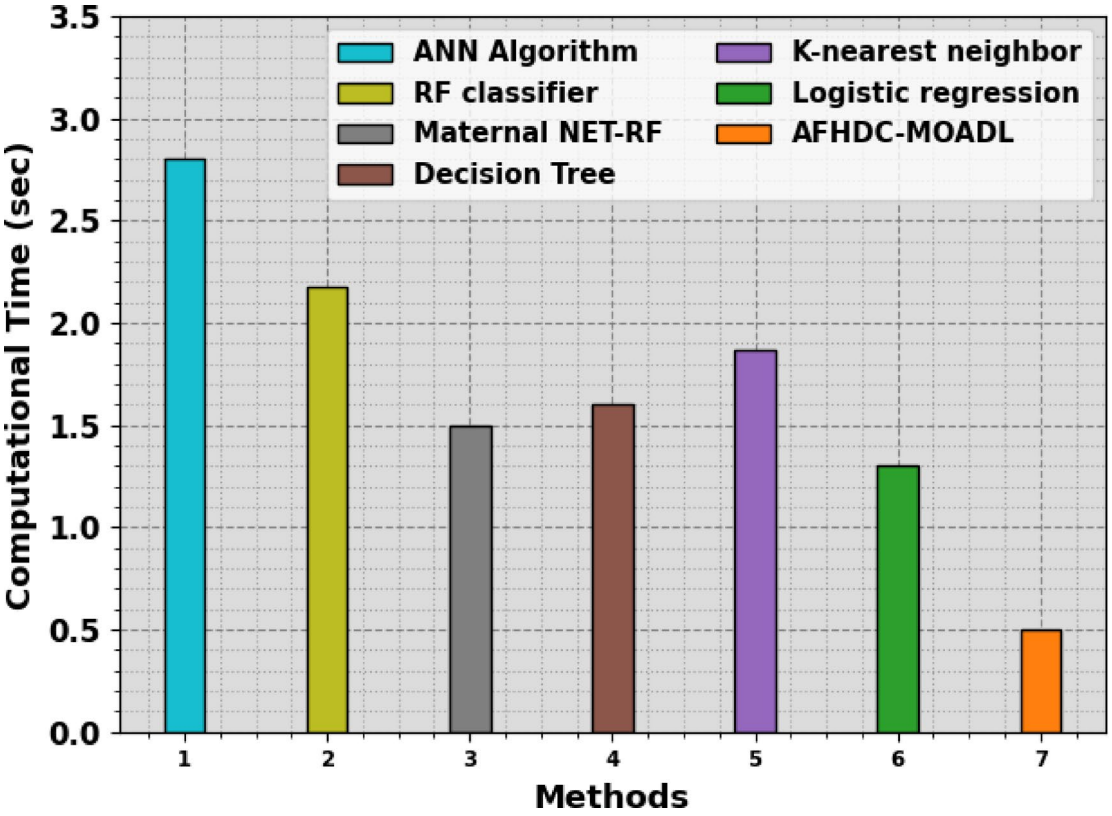

Fig. 10. CT outcome of AFHDC MOADL technique with existing approaches.

Configuration	Accuracy (%)	Precision (%)	Sensitivity (%)	F1 score (%)	ROC AUC (%)
Full AFHDC MOADL (MOA + GCN + RMSProp)	**98.12**	**96.86**	**94.34**	**95.40**	**99.80**
Without MOA	94.62	93.10	90.02	91.90	97.42
Without RMSProp optimization	95.31	94.08	91.40	92.60	98.10
GCN replaced with MLP	93.84	92.21	89.15	90.40	96.55

Table 5. Ablation study for the proposed AFHDC MOADL method.

Data availability

https://www.kaggle.com/datasets/andrewmvd/fetalhealthclassification.

Received: 19 February 2025; Accepted: 1 October 2025
Published online: 06 November 2025

References

1. Frasch, M. G., Strong, S. B., Nilosek, D., Leaverton, J. & Schifrin, B. S. Detection of preventable fetal distress during labor from scanned cardiotocogram tracings using deep learning. *Front. Pediatr.* **9**, 736834 (2021).
2. Krupa, A. J. D., Dhanalakshmi, S., Lai, K. W., Tan, Y. & Wu, X. An IoMT enabled deep learning framework for automatic detection of fetal QRS: A solution to remote prenatal care. *J. King Saud Univ. Comput. Inf. Sci.* **34**(9), 7200–7211 (2022).
3. Cao, Z. et al. Intelligent antepartum fetal monitoring via deep learning and fusion of cardiotocographic signals and clinical data. *Health Inf. Sci. Syst.* **11**(1), 16 (2023).
4. Priya, M. & Nandhini, M. Detection of fetal brain abnormalities using data augmentation and convolutional neural network in the internet of things. *Meas. Sensors* 100808 (2023).
5. Sreelakshmy, R. et al. An automated deep learning model for the cerebellum segmentation from fetal brain images. *BioMed Res. Int.* (2022).
6. Krishna, T. B. & Kokil, P. Automated classification of common maternal fetal ultrasound planes using multi layer perceptron with deep feature integration. *Biomed. Signal Process. Control*, **86**, 105283 (2023).
7. Deepika, P., Suresh, R. M. & Pabitha, P. Defending Against Child Death: Deep learning-based diagnosis method for abnormal identification of fetus ultrasound Images. *Comput. Intell.* **37**(1), 128–154 (2021).
8. Vahedifard, F. et al. Automatic ventriculomegaly detection in fetal brain MRI: A step by step deep learning model for novel 2D 3D linear measurements. *Diagnostics* **13**(14), 2355 (2023).
9. Boudet, S., Houzé de l'Aulnoit, A., Peyrodie, L., Demailly, R. & Houzé, D. Use of Deep Learning to Detect the Maternal Heart Rate and False Signals on Fetal Heart Rate Recordings. *Biosensors* **12**(9), 691 (2022).

10. Einy, S., Sen, E., Saygin, H., Hivehchi, H. & Dorostkar Navaei, Y. Local Binary Convolutional Neural Networks' Long Short Term Memory Model for Human Embryos' Anomaly Detection. *Sci. Program.* (2023).
11. Addanke, S. & Anandan, R. Original research Article secure IoT based smart system for monitoring health care for ambulatory and fetal. *J. Auton. Intell.* **7**(3). (2024).
12. Edupuganti, M., Rathikarani, V. & Chaduvula, K. A Real and Accurate Ultrasound Fetal Imaging Based Heart Disease Detection Using Deep Learning Technology. *Int. J. Integr. Eng.* **14**(7), 56–68 (2022).
13. Krishna, T. B. & Kokil, P. Standard fetal ultrasound plane classification based on stacked ensemble of deep learning models. *Expert Syst. Appl.* **238**, 122153 (2024).
14. Gupta, K., Bajaj, V. & Ansari, I. A. Integrated s transform based learning system for detection of arrhythmic fetus. *IEEE Trans. Instrum. Meas.* (2023).
15. Zeng, Y., Zhang, R., Zhang, H., Qiao, S., Huang, F., Tian, Q., & Peng, Y. GCCNet: A novel network leveraging gated cross correlation for multi view classification. *IEEE Trans. Multimedia* **27**, 1086–1099. https://doi.org/10.1109/TMM.2024.3521733 (2025).
16. Hu, F., Yang, H., Qiu, L., Wei, S., Hu, H., & Zhou, H. Spatial structure and organization of the medical device industry urban network in China: Evidence from specialized, refined, distinctive, and innovative firms. *Front. Public Health* **13**, 1518327. https://doi.org/10.3389/fpubh.2025.1518327 (2025).
17. Qiu, W. et al. Federated abnormal heart sound detection with weak to no labels. *Cyborg Bionic Syst.* **5**, 0152. https://doi.org/10.34133/cbsystems.0152 (2024).
18. Qian, K. et al. Learning representations from heart sound: A comparative study on shallow and deep models. *Cyborg Bionic Syst.* **5**, 0075. https://doi.org/10.34133/cbsystems.0075 (2024).
19. Ma, N., Fang, X., Zhang, Y., Xing, B., Duan, L., Lu, J., & Ma, D. Enhancing the sensitivity of spin exchange relaxation free magnetometers using phase modulated pump light with external Gaussian noise. *Optics Express* **32**(19), 33378–33390. https://doi.org/10.1364/OE.530764 (2024).
20. Bing, P., Liu, W., Zhai, Z., Li, J., Guo, Z., Xiang, Y., & Zhu, L. A novel approach for denoising electrocardiogram signals to detect cardiovascular diseases using an efficient hybrid scheme. *Front. Cardiovasc. Med.* **11**, 1277123. https://doi.org/10.3389/fcvm.2024.1277123 (2024).
21. Zhang, Z., Wu, K., Wu, Z., Xiao, Y., Wang, Y., Lin, Q., & Liu, Q. A case of pioneering subcutaneous implantable cardioverter defibrillator intervention in Timothy syndrome. *BMC Pediatr.* **24**(1), 729. https://doi.org/10.1186/s12887024-05216-w (2024).
22. Bilal, A., Shafiq, M., Obidallah, W. J., Alduraywish, Y. A. & Long, H. Quantum computational infusion in extreme learning machines for early multi cancer detection. *J. Big Data.* **12** (1), 1–48 (2025).
23. Attar, H. et al. B5G applications and emerging services in smart IoT environments. *Int. J. Crowd Sci.* **9** (2), 79–95. https://doi.org/10.26599/IJCS.2024.9100007 (2025).
24. https://www.kaggle.com/datasets/andrewmvd/fetalhealthclassification.

Author contributions

K.N; Conceptualization, K.N; Data curation, K.R; Formal Analysis, K.R; Investigation, K.R; Methodology, K.N; Writing, K.R; validation, K.R; investigation.

Declarations

Competing interests

The authors declare no competing interests.

Additional information

Correspondence and requests for materials should be addressed to K.N.

Reprints and permissions information is available at www.nature.com/reprints.

Publisher's note Springer Nature remains neutral with regard to jurisdictional claims in published maps and institutional affiliations.